References

[1] Gardon, R., "An Instrument for the Direct Measurement of Thermal Radiation," *Review of Scientific Instruments*, Vol. 24, May 1953, pp. 366–370.

[2] Malone, E. W., "Design and Calibration of Thin Foil Heat Flux Sensors," Paper P6-2-PHYMMID-67, 1967, Instrument Society of America.

[3] Woodruff, L. W., Hearne, L. F., and Keliher, T. J., "Interpretation of Asymptotic Calorimeter Measurements," *AIAA Journal*, Vol. 5, No. 4, April 1967, pp. 795–797.

Stability and Shape of Magnetically Balanced Cross-Flow Arcs

DAVID M. BENENSON* AND ALLEN J. BAKER†

State University of New York at Buffalo, Buffalo, N.Y.

EXPERIMENTAL investigations of the magnetically balanced cross-flow arcs have been reported in Refs. 1 and 2. In Ref. 1, the arc (about 5-in. length) was drawn between a thoriated tungsten cathode and a copper, coil-type anode; the electrodes were placed outside the test section. Instability occurred at speeds of about 60 ft/sec. Generally, the instability was associated with erratic behavior at the anode attachment, resulting in electrode failure (Ref. 3). Tests reported in Ref. 2 were conducted upon rail and pointed electrode configurations (electrode spacing in each case was $\frac{1}{2}$ in.); all electrodes were copper. Arc instability was followed by extinction of the arc (Ref. 4). For the pointed electrodes configuration, instability was reached at about 50 ft/sec; with rail electrodes, instability occurred at about 130 ft/sec. For both Refs. 1 and 2, visual observation of the arc was generally confined to views transverse (i.e., normal, $\alpha = 0°$) to the flow (and arc) and from the downstream direction ($\alpha = 90°$). The ratio $\bar{L}$ (characteristic dimension transverse to the flow to that in the direction of flow) was found to be of the order 1–2 (Ref. 1). This ratio was probably about the same for the rail electrode configuration of Ref. 1, even though the plasma was bulbous near one of the electrodes; comparable information for the pointed electrode configuration was not reported.

Our experience with similar plasma configurations suggests that the occurrence of such instabilities or of arc oscillations under supposedly steady-state operation (Ref. 5) may depend upon many factors (additional to velocity and arc current), including the electrode configuration, electrode material, and tunnel geometry.

Reported herein are results of tests conducted upon magnetically balanced, atmospheric, cross-flow arcs in argon. Electrodes of the pointed type were used: 90° conical tip, 0.250-in.-base-diam copper anode and a 0.080-in.-diam, 0.469-in.-long tantalum cathode. The arrangement was placed inside a $1\frac{7}{8}$-in. × $1\frac{7}{8}$-in. test section; electrode spacings were in the range $\frac{1}{4}$–$\frac{1}{2}$ in. Arc currents up to 150 amp were employed. Transverse magnetic field, uniform to within ±0.15% in a 1-in.[3] volume centered about the electrode centerline and duct centerline, was applied using a coil arrangement; field strengths in excess of 500 gauss were developed. The field arrangement permitted observation of the plasma over a wide range of azimuthal angles [with such an arrangement, the temperature distribution within the plasma will be obtained employing techniques previously developed for nonmagnetically balanced cross-flow arcs (Refs. 6, 7)].

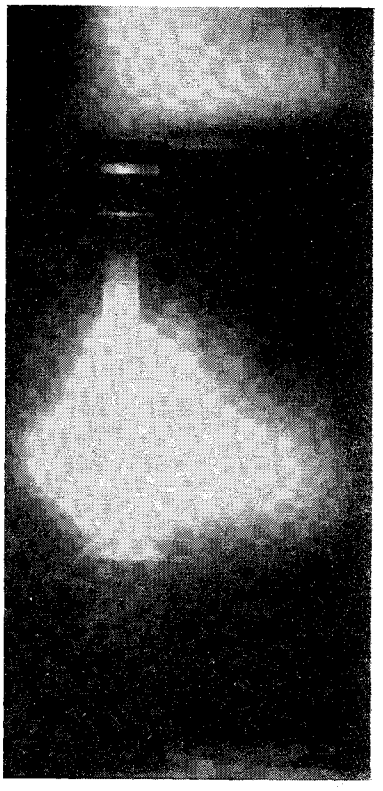

Fig. 1 Arch attachments on downstream side of electrodes: cathode over anode; $\alpha = 45°$, $U = 10.4$ fps, $I = 132$ amp, electrode spacing = 0.500 in., and $B = 18$ gauss.

Tests were carried out to velocities of about 81.5 ft/sec. Instability did not occur. Fluctuation of the central portion of the column became more pronounced at the higher velocities; the amplitude of the fluctuations was of the order of the arc dimension in the direction of flow. In all tests both anode and cathode attachment appeared fixed, i.e., steady-in position.

Two different types of balanced arc modes have been found, the configurations observed depending upon whether the plasma attachments were on the upstream or the downstream (or at the apex) side of the electrode. In turn, the location of the attachment points depended upon the velocity as well as upon the strength of the transverse magnetic field (i.e., the $\bar{J} \times \bar{B}$ body force). In fact, a critical or threshold velocity was found, below which the magnetic field available was not sufficient to force the attachment points onto the upstream side of the electrodes. Below this critical velocity, the magnetic field appeared to affect primarily the arc column. With sufficient field, the column was forced relatively far upstream; under these conditions, the plasma appeared distinctly filamentary.

As expected, for a given current and velocity, the arc may be operated in a stable mode over a wide range of magnetic fields. Under these conditions, a configuration is obtained which generally is no longer colinear (or nearly colinear) with the electrodes (i.e., no longer balanced); the resulting cusp-shaped appearance is similar to that studied previously for nonmagnetically balanced cross-flow plasmas.[6,7]

With balanced operation and with the arc attachments at the apex or on the downstream side of the electrodes, $\bar{L}$ was generally relatively large, of the order of 3–5 [Fig. 1; all photographs were taken using a narrow band (10 Å) optical interference filter centered at 4454 Å.] In comparison, plasma attachments on the upstream side of the electrode resulted in a relatively longer plasma in which the characteristic transverse dimension was of the same magnitude as the characteristic axial dimension ($\bar{L} \sim 1$–2; Figs. 2, 3).

Received April 30, 1969. This research was supported by the National Science Foundation Grant GK-1174.

* Professor, Faculty of Engineering and Applied Sciences. Associate Fellow AIAA.

† Instructor, Faculty of Engineering and Applied Sciences.

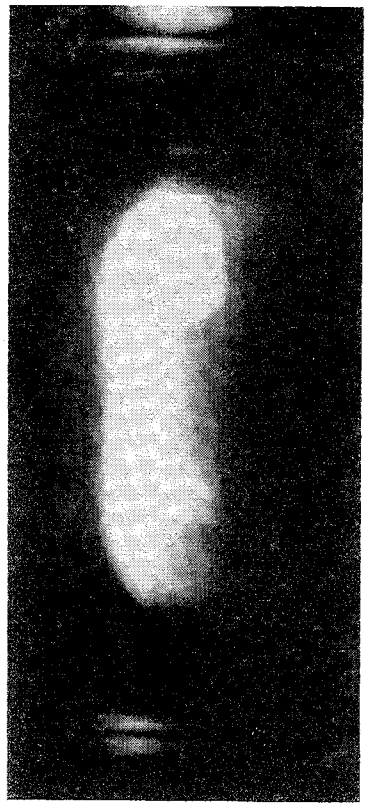

Fig. 2 Arc attachments on upstream side of electrodes: cathode over anode; $\alpha = 0°$, flow from left to right; $U = 16.7$ fps, $I = 132$ amp, electrode spacing = 0.500 in., and $B = 108$ gauss.

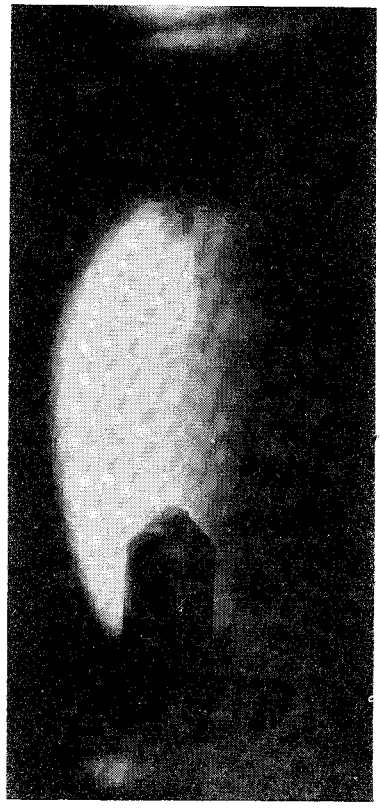

Fig. 3 Arch attachments on upstream side of electrodes: cathode over anode; $\alpha = 45°$, $U = 16.7$ fps, $I = 132$ amp, electrode spacing = 0.500 in., and $B = 108$ gauss.

A balanced configuration was achieved starting generally from the cusp-shaped configuration noted earlier. The attachments were located on the downstream side of the electrodes. An increase in magnetic field strength resulted in greater deflection of the arc column than in motion of the attachment points. At the balanced condition, the attachments would be located at or close to the apex of the electrodes; as noted previously, the value of $\bar{L}$ was large, in the range 3–5. Above the critical velocity, further increase in field strength would drive the arc attachments onto the upstream side of the electrodes. Following this, the arc would lengthen along the electrodes (Fig. 2) and the value of $\bar{L}$ would be reduced to the range 1–2. Below the critical velocity, increasing the field strength beyond that required for balance caused the arc column to be forced upstream. The column could very easily be driven upstream the equivalent of several electrode spacings; the filamentary appearance would be observed under these conditions. Arc attachments could not be driven onto the upstream side of the electrodes with the magnetic field strengths available.

With the arc subject to the transverse magnetic field and in the cusp-shaped configuration, the $\bar{J} \times \bar{B}$ body force contains, at the simplest (assuming a uniform transverse magnetic field and the column to be both vertically oriented and symmetrical about a horizontal plane located midway between the electrodes), two components: 1) upstream, in the horizontal direction and 2) a vertical component, directed downward, acting upon the column located above the horizontal plane of symmetry and a vertical component directed upward, acting upon the column located below the horizontal plane of symmetry. The magnitude of the components will vary along the plasma in relation to the local size and direction of the column (i.e., to $\bar{J}$). The effect of the body force is both to drive the column upstream and to force (squeeze) the upper and lower portions toward each other; this evidently results in a spreading of the column in the transverse direction.

The relatively large dimension in the transverse direction and the relative ease with which the column can be moved with respect to the arc attachments suggests that 1) the temperature within a cross section (taken in a horizontal plane) may be relatively high in a fairly narrow region (core) near the center, i.e., most of the current may be carried by a relatively small portion of the plasma 2) as the plasma is forced into the balanced mode from a cusp-shaped configuration, the core region increases in temperature such that current density becomes larger, and 3) temperature over much of the large transverse region is relatively low compared to that within the core. Techniques previously developed[6,7] will be used to diagnose this aspect.

Once the attachment points are forced onto the upstream side of the electrodes, the vertical components of the magnetic body force tend to pull apart (or stretch) the upper and lower portions of the plasma. This effect would lead to a longer plasma, one which would tend to be much smaller in transverse dimension than the configuration which occurs when the attachments are on the downstream side of the electrodes.

The existence of a critical velocity, as described earlier, suggests that convection may influence the current densities to a greater extent within the electrode regions than in the column. Results of Refs. 6 and 7 and extensions thereof indicate a profound effect of velocity upon the temperature distribution within the plasma. Following balance, then, when above the critical velocity, an increase in magnetic field could drive the attachment points onto the upstream side of the electrodes. It is speculated that, below the critical velocity, continued increase of the field beyond that required for balance may result in continuing decrease in current density. It is necessary to obtain quantitative measurements near the electrodes and within the column in order to describe accurately the phenomena observed.

References

[1] Roman, W. C. and Myers, T. W., "Experimental Investigation of an Electric Arc in Transverse Aerodynamic and Magnetic Fields," *AIAA Journal*, Vol. 5, No. 11, Nov. 1967, pp. 2011–2017.

[2] Winograd, Y. Y. and Klein, J. F., "Electric Arc Stabilization in Crossed Convective and Magnetic Fields," AIAA Paper 68-709, Los Angeles, Calif., 1968.

[3] Roman, W. C., private communication.
[4] Klein, J. F., private communication.
[5] Benenson, D. M., Naeher, C. H., and Gideon, J. B., "Oscillations of Electric Arcs in Argon Cross-Flow," *AIAA Journal*, Vol. 5, No. 8, Aug. 1967, pp. 1517–1519.
[6] Benenson, D. M., Baker, A. J., and Cenkner, A. A., Jr., "Diagnostics on Steady-State Cross-Flow Arcs, I. Low Current," ARL 68-0109, 1968, Aerospace Research Labs., Office of Aerospace Research.
[7] Benenson, D. M., Baker, A. J., and Cenkner, A. A., Jr., "Diagnostics on Steady-State Cross-Flow Arcs," *IEEE Transactions on Power Apparatus and Systems*, Vol. PAS-88, May 1969, pp. 513–521.

Average Relative Velocity of Sporadic Meteoroids in Interplanetary Space

Donald J. Kessler*
NASA Manned Spacecraft Center, Houston, Texas

Introduction

THE orbital elements obtained from more than 2000 sporadic meteors listed by McCrosky and Posen[1] can, with certain assumptions, be used to determine the meteoroid velocity distribution relative to a body in orbit around the sun. The purpose of this Note is to determine the average velocity of meteoroids relative to a spacecraft having any specified velocity and position in space.

Correction of Data to a Limiting Mass

Before any velocity calculations are made, the meteor sample must be corrected to some limiting mass. The major selection effects can easily be considered by the following procedure.

Assuming that the number of meteors in Ref. 1 can be expressed by

$$N \propto I_f^{-\beta} n_f(v_\infty) \tag{1}$$

where I_f is the maximum intensity of the meteor as recorded on the film, and $n_f(v_\infty)$ is the number of meteors with velocities between v_∞ and $v_\infty + dv_\infty$, and v_∞ is the accelerated velocity of the meteor at the instant the meteor enters the atmosphere of the earth.

The maximum intensity of a meteor is given by Ref. 2 as

$$I_{\max} \propto m^{0.9} v_\infty^{3.5} \tag{2}$$

where m is the initial meteor mass. Then, the intensity of the meteor as recorded on the film will be

$$I_f \propto I_{\max}/v_a h^2 \tag{3}$$

where v_a is the angular velocity of the meteor and h is the altitude of the meteor above the observation station. Assuming that the radiant distribution of the meteors is independent of the velocity and intensity distributions

$$v_a \propto v_\infty/h \tag{4}$$

Reference 3 relates v_∞ to h by

$$h \propto v_\infty^{0.25} \tag{5}$$

The number of meteors per unit area will vary as

$$F \propto N/h^2 \tag{6}$$

Received May 2, 1969.
* Aerospace Technologist, Meteoroid Sciences Branch.

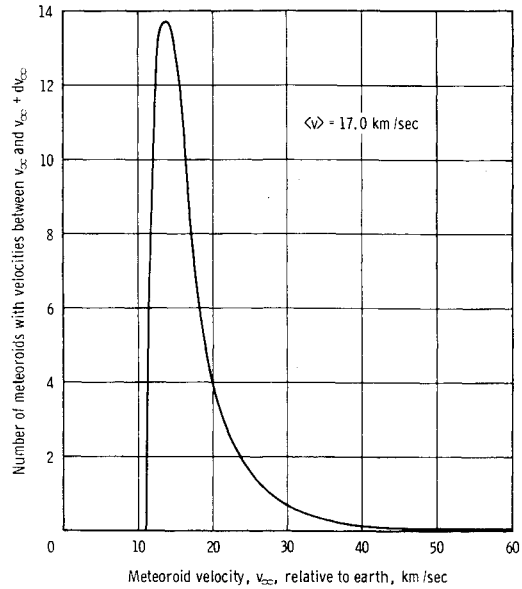

Fig. 1 Meteoroid velocity distribution relative to earth, after gravitational attraction.

Thus, combining Eqs. (1) to (6), the flux as a function of mass and velocity will vary as

$$F \propto m^{-0.9\beta} n_f(v_\infty)/v^{2.5\beta + 0.25(2-\beta)} \tag{7}$$

Therefore

$$n_m(v_\infty) = n_f(v_\infty)/v^{2.5\beta + 0.25(2-\beta)} \tag{8}$$

where $n_m(v_\infty)$ is the velocity distribution to some limiting mass.

Reference 4 gives the value of β as 1.34, so that the weighting factor becomes $v_\infty^{-3.5}$. Although the method of obtaining the weighting factor of $v_\infty^{-3.5}$ is simplified, this factor can be shown to be equivalent to using the more precise method of velocity-distribution correction used by Dohnanyi.[5] The results differ slightly because Dohnanyi found $N \propto m^{-1}$ (i.e., $\beta = 1/0.9$) and did not consider v_∞ as a function of h.

The data for the sporadic meteors in Ref. 1 were put on magnetic tape and a computer program was written to obtain $n_m(v_\infty)$. The results are shown in Fig. 1, with an average velocity of 17.0 km/sec.

Velocity Distribution Relative to a Massless Earth

Since the earth "pulls in" more slowly moving meteoroids, each meteor must be weighted by v_G^2/v_∞^2 (as given in Ref. 6)

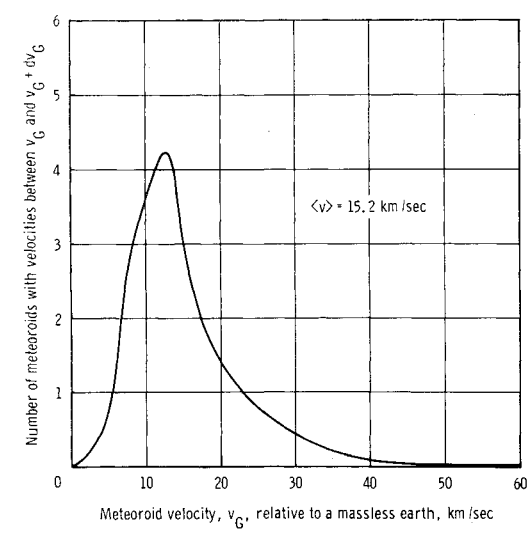

Fig. 2 Meteoroid velocity distribution relative to earth, before gravitational attraction.